Eur. Phys. J. B **34**, 135–142 (2003)
DOI: 10.1140/epjb/e2003-00205-5

THE EUROPEAN PHYSICAL JOURNAL B

Influence of temperature on the nodal properties of the longitudinal thermal conductivity of $YBa_2Cu_3O_{7-x}$

R. Ocaña and P. Esquinazi[a]

Abteilung Supraleitung und Magnetismus, Institut für Experimentelle Physik II, Universität Leipzig, Linnéstr. 5, 04103 Leipzig, Germany

Received 10 September 2002 / Received in final form 7 March 2003
Published online 4 August 2003 –

Abstract. The angle dependence at different temperatures of the longitudinal thermal conductivity $\kappa_{xx}(\theta)$ in the presence of a planar magnetic field is presented. In order to study the influence of the gap symmetry on the thermal transport, angular scans were measured up to a few Kelvin below the critical temperature T_c. We found that the four-fold oscillation of $\kappa_{xx}(\theta)$ vanishes at $T > 20$ K and transforms into a one-fold oscillation with maximum conductivity for a field of 8 T applied parallel to the heat current. Nevertheless, the results indicate that the $d-$wave pairing symmetry remains the main pairing symmetry of the order parameter up to T_c. Numerical results of the thermal conductivity using an Andreev reflection model for the scattering of quasiparticles by supercurrents under the assumption of $d-$wave symmetry provide a semiquantitative description of the overall results.

PACS. 74.25.Fy Transport properties (electric and thermal conductivity, thermoelectric effects, etc.) – 74.72.Bk Y-based cuprates – 72.15.-v Electronic conduction in metals and alloys

1 Introduction

The order parameter in high-temperature superconductors (HTS) has been proved to have mainly a $d_{x^2-y^2}$ pairing symmetry [1–4]. In particular, try-crystal phase-sensitive measurements [1] have determined the presence of a predominant $d_{x^2-y^2}-$gap symmetry up to the superconducting critical temperature T_c over, if any, other minor components smaller than 5% of that with the $d_{x^2-y^2}-$symmetry. Thermal transport measurements have also shown the predominance of this symmetry for the gap function. In particular, when a magnetic field is rotated parallel to the CuO_2 planes, the longitudinal thermal conductivity shows a fourfold oscillation which can be explained in terms of both Andreev scattering of quasiparticles by vortices (AS) and Doppler shift (DS) in the energy spectrum of the quasiparticles if one takes a $d_{x^2-y^2}-$gap into account [2–4]. Nevertheless, the fourfold oscillation in the thermal conductivity has been resolved up to ~ 15 K. Above this temperature, no direct evidence for this type of symmetry from this kind of measurements has been published. Furthermore, deviations from the expected angular pattern within a pure $d_{x^2-y^2}-$symmetry have been attributed to the effect of pinning of vortices [2].

The variation of the thermal conductivity as a function of angle θ between the heat current and the magnetic field applied parallel to the CuO_2 planes depends mainly on the heat transport by quasiparticles, their interaction with the supercurrents (vortices) and the symmetry of the order parameter [2–4]. An angular pattern showing properties of the order parameter symmetry can only be achieved when the temperature is low enough so that the quasiparticle momentum is close to the nodal directions of the gap. Otherwise, thermal activation would also induce quasiparticles at different orientations from those of the nodes and hence, the sensitivity of the probe to measure gap characteristics will be reduced. The first question we address in this paper is related to the temperature range at which the nodal characteristics of the gap are directly observable by thermal conductivity. The second question we would like to clarify in this paper is whether the thermal activation of quasiparticles with increasing temperature, treated phenomenologically within a Fermi liquid approximation for thermal transport including the $d_{x^2-y^2}-$gap function, can explain the experimental results in the whole temperature range, in particular the change of symmetry of $\kappa_{xx}(\theta)$ as a function of temperature. In this paper, we calculate numerically the thermal conductivity at different angles and temperatures at fixed magnetic field,

[a] e-mail: esquin@physik.uni-leipzig.de

assuming an Andreev reflection model for the scattering of quasiparticles by supercurrents, originally proposed by Yu *et al.* [5–7] within the two dimensional BRT expression [8] for the thermal conductivity, and compare it to the experimental data.

Angle scans in a magnetic field applied parallel to the CuO_2 planes were performed in order to measure the angular variation of the longitudinal thermal conductivity $\kappa_{xx}(\theta)$ in two single crystals of $YBa_2Cu_3O_{7-x}$ high-temperature superconductor. The overall results agree with the theoretical model and confirm the predominance of the $d_{x^2-y^2}-$gap up to T_c. The measurements provide also new results that improve our knowledge of the thermal transport at temperatures at which the nodal properties of the gap are not directly observable.

Following the experimental and sample details of the next section, we present in Section 3 the main experimental results. In Section 4 we describe the used model and compare it with the experimental data. A brief summary is given in Section 5.

2 Experimental and sample details

In order to rule out effects concerning shape and structure characteristics of the crystal we have used two different samples of $YBa_2Cu_3O_{7-x}$ (YBCO): a twinned single crystal with dimensions (length × width × thickness) $0.83 \times 0.6 \times 0.045\ \mathrm{mm}^3$ and critical temperature $T_c = 93.4$ K previously studied in references [9–11,4] and an untwinned single crystal with dimensions $2.02 \times 0.68 \times 0.14\ \mathrm{mm}^3$ and $T_c = 88$ K [11]. For the measurement of the thermal conductivity, a heat current J was applied along the longest axis of the crystal studied. In the untwinned sample, J was parallel to the a-axis and in the twinned crystal was parallel to the a/b-axes (twin planes oriented along (110)). In both cases the position of the lattice axis with respect to the crystal axis was determined using polarized light microscopy and X-ray diffraction.

The longitudinal temperature gradient ($\nabla_x T$) was measured using previously calibrated chromel-constantan (type E) thermocouples [12] and a dc picovoltmeter. Special efforts were made in order to minimize the misalignment of the plane of rotation of the magnetic field applied perpendicular to the c-axis with the CuO_2 planes of the sample. This misalignment was minimized step by step, measuring the angle dependence of $\kappa_{xx}(\theta)$ until a satisfactory symmetrical curve was obtained. In this way, we estimate a misalignment smaller than 0.5°. An *in situ* rotation system enabled measurement of the thermal conductivity as a function of the angle θ defined between the applied field and the heat flow direction along $+\widehat{x}$, see Figure 1. For more details on the experimental arrangement see reference [4].

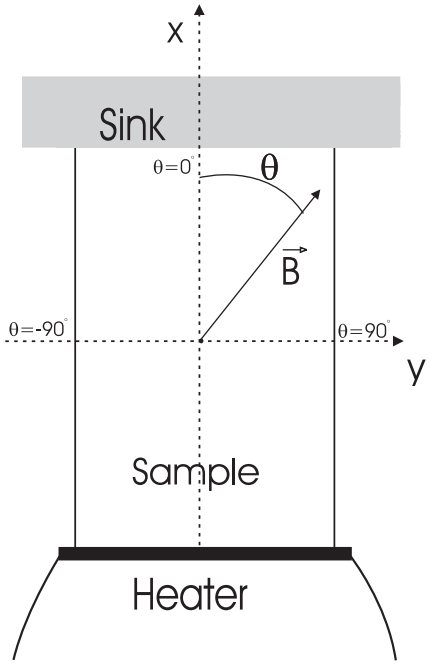

Fig. 1. Top view of the sample arrangement and the definition of the angle θ.

As pointed out by Aubin *et al.* [2] and observed in references [9,4], the effect of the pinning of vortices plays an important role in determining the correct angle pattern in this kind of measurement. In fact, when the angle of the magnetic field is changed, a non uniform vortex distribution due to pinning forces may appear. As argued in reference [4], the pinning of the Josephson-like vortices parallel to the planes is strongly affected by vortices perpendicular to the planes which may appear due to the misalignment of the crystal axes with respect to the applied magnetic field. In this situation, even hysteresis in the angular patterns of the thermal conductivity can be measured [2]. We note that pinning of vortices is influenced by the distribution of the oxygen vacancies in the sample as well as by defects and impurity centers. Thus, in order to rule out the influence of this effect in the measurements, a field-cooled procedure have to be used. This procedure consists of two steps. In the first step the sample is driven into the normal state by heating to a few Kelvin above T_c and the angle is changed. Secondly, it is cooled down to the desired temperature at constant field.

In Figure 2 we show the longitudinal thermal conductivity as a function of the temperature in both crystals at zero magnetic field. As argued by many authors (see for example references [13–15]), the observed behavior in Figure 2 provides qualitative information about the quality of the sample. The height of the peak observed in the temperature dependence of the thermal conductivity is related

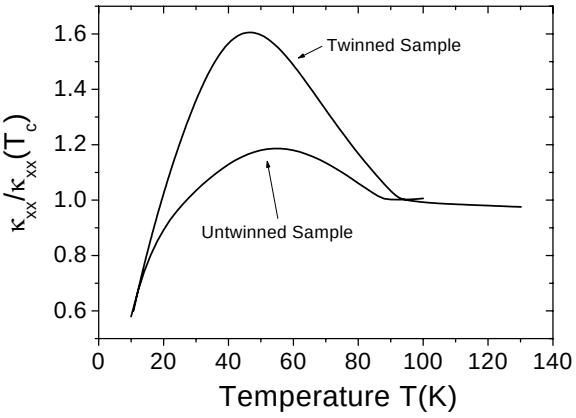

Fig. 2. Temperature dependence of the longitudinal thermal conductivity κ_{xx} for the twinned and untwinned crystals. The curves are normalized by the value of the thermal conductivity at T_c. Within $\sim$ 30% error the absolute value of the thermal conductivity at T_c for the untwinned (twinned) crystal is $\kappa_{xx}(T_c) \simeq 12(8)$ W/Km.

to the relative contributions between the density of impurity scattering centers and the strength of the inelastic electron-electron scattering. Crystals showing large peaks may have a small amount of impurity scattering centers [16] and/or larger quasiparticle-related inelastic contribution. The origin of the peak is explained in terms of a competition between the decrease of the inelastic scattering rate [17] and the decrease of the population of quasiparticles as temperature decreases [14,18,19]. Taking this into account we might conclude that the untwinned crystal has a larger impurity scattering and a smaller quasiparticle-related inelastic scattering since its peak is considerably smaller than that of the twinned sample. This is supported by its reduced T_c with respect to the twinned sample (which indicates a larger density of oxygen vacancies). Since the thermal conductivity at T_c appears to be larger for the untwinned sample, we conclude that there should be a substantial reduction of the inelastic scattering. As we show below, this makes the measurement of electronic properties related to the gap symmetry more difficult.

3 Experimental results and discussion

The angular patterns of the longitudinal thermal conductivity κ_{xx} at different temperatures for the twinned and untwinned crystals are shown in Figures 3 and 4 respectively. At low enough temperatures ($T < 20$ K), a magnetic field parallel to the CuO_2 planes of the sample produces a fourfold oscillation in the longitudinal thermal conductivity as the field is rotated from $\theta = 90°$ to $\theta = -90°$. We note that at both $\theta = 90°$ and $\theta = -90°$ the magnetic field is perpendicular to the heat

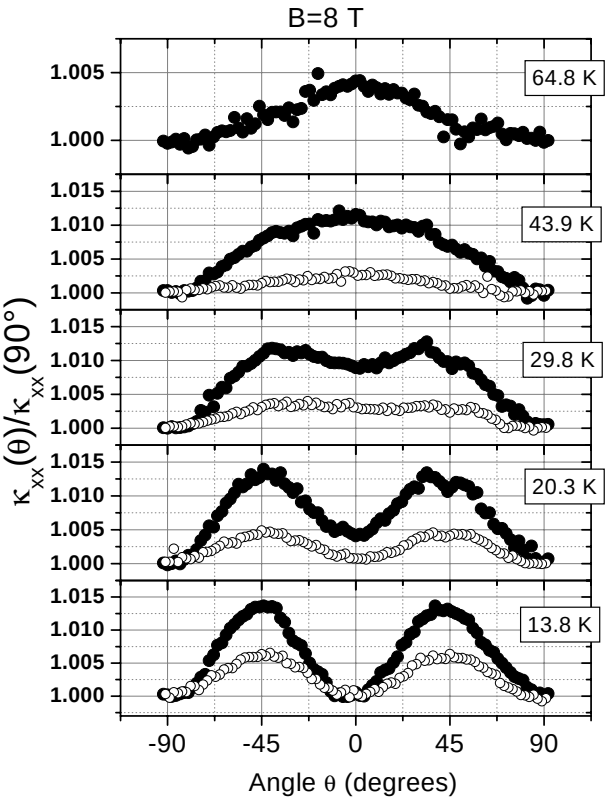

Fig. 3. Angle dependence of the longitudinal thermal conductivity at different temperatures for the twinned sample. The results are normalized to the value of the thermal conductivity at $\theta = 90°$, when the field was applied perpendicular to the heat current. Solid circles are taken in a magnetic field strength of 8 T and open circles at 3 T.

flow. At $\theta = 0°$ the field is parallel to the heat flow (see Fig. 1). As noted in references [2] and [4] the angular patterns are not free of the phononic contribution to the total thermal conductivity. However, this contribution seems to be constant under variations of the magnetic field orientations for two reasons. 1) For fields parallel to the CuO_2 planes, vortices are unlikely to have a normal core (Josephson vortices), making a change of the phonon attenuation with field and angle unlikely. 2) There is no experimental evidence that the phononic contribution does change substantially with field. The similarity between the temperature dependencies of κ_{xx} and κ_{xy} below T_c where a large change in the quasiparticle density ocurrs [10], indicates that the phonon-electron interaction does not play a main role in the temperature dependence of κ. The electronic contribution is entirely responsible for the magnetic field dependence, revealed in both thermal conductivity [20–22,10] and in microwave measurements [17], and indicates against any large phonon-electron scattering. In fact, no remarkable

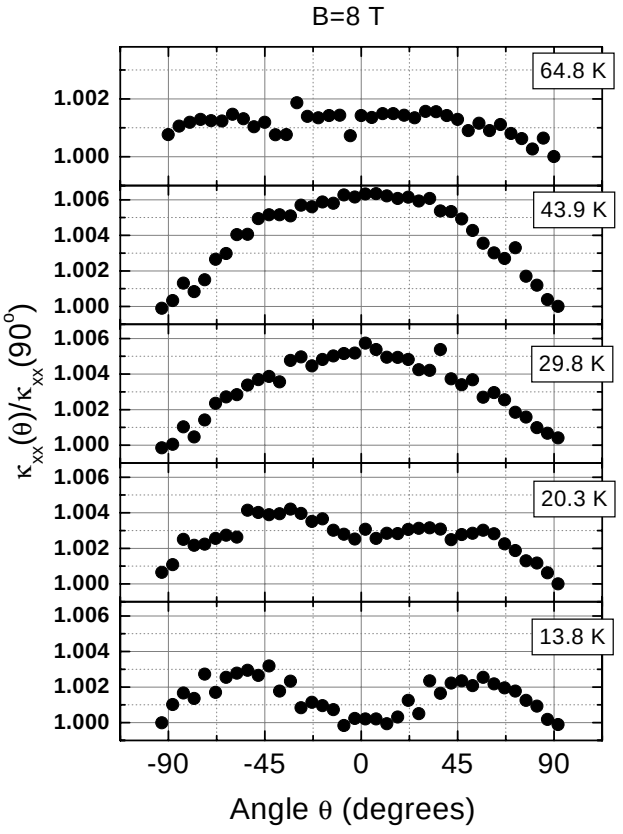

Fig. 4. Angle dependence patterns of the longitudinal thermal conductivity at different temperatures and 8 T for the untwinned sample. The results are normalized to the value of the thermal conductivity when the field was applied perpendicular to the heat current, at $\theta = 90°$.

phonon-electron scattering have been addressed in those experiments where the measured magnetic field dependencies are larger than the oscillation amplitudes measured in this paper. Therefore, measurable contributions of the phonons *via* phonon-electron scattering are more unlikely to occur in the angular patterns. This characteristic makes the angular profiles of the thermal conductivity suitable to be compared with electronic models by using the quantity $\kappa_{xx}(\theta) - \kappa_{xx}(90°)$ where the phononic contribution is subtracted [4].

As pointed out in reference [4], the variation of the thermal conductivity in Figures 3 and 4 can be explained with a model involving a Doppler shift (DS) in the energy spectrum of the quasiparticles along with an accurate inclusion of the impurity scattering [23,24,14,15] and/or assuming Andreev scattering (AS) of quasiparticles by vortices [5]. Briefly, in the mixed state the quasiparticles are in the presence of a phase gradient produced by the superfluid flow of the vortices. Thus, as viewed from the laboratory frame they experience a Doppler shift in their energy spectrum given by the scalar product of the momentum and superfluid velocity, $\mathbf{p}\cdot\mathbf{v}_s$. When a quasiparticle of momentum $\mathbf{p}$ is moving parallel to the magnetic field, the product is zero and hence, no DS occurs. Thus, the angular characteristic of this effect is to produce an excess of quasiparticles in the direction perpendicular to the field and thereby, reducing the "local" thermal resistance at this orientation [23,24,14]. When the field is placed parallel to the heat current, the Doppler shift is the same for both nodal directions at $\theta = 45°$ and $\theta = -45°$. Therefore and since thermal resistances must be added in parallel, a simple picture in which there are only quasiparticles at the nodes would produce a fourfold oscillation in the thermal conductivity with opposite sign to that observed in the measurements. However, as pointed out in references [15,14,24], the DS affects both the carrier density as well as the scattering rate of quasiparticles, and since at high enough temperatures the latter dominates, the quasiparticles move more easily parallel to the magnetic field. Therefore, the sign of the fourfold oscillation observed in the experiments is also recovered within this picture.

In the AS mechanism a phase gradient, namely, the superfluid flow surrounding the vortices may induce Andreev reflection of the quasiparticles [25]. Thus, the DS in the energy spectrum $\mathbf{p}\cdot\mathbf{v}_s$ is implicitly taken into account in the AS picture. As viewed from the laboratory frame, when the quasiparticle energy equals the value of the gap, then the quasiparticle is transformed into a quasihole reversing its velocity and hence, decreasing its contribution to the thermal conductivity. Thus, a quasiparticle with momentum $\mathbf{p}$ parallel to the magnetic field does not experience a DS and hence, no Andreev reflection can take place. The field acts as a filter [26] for the quasiparticle that contributes to reduce the total temperature gradient. Note that the AS picture gives rise to a fourfold oscillation in the thermal conductivity as the magnetic field is rotated parallel to the CuO_2 planes without more considerations.

Then, qualitatively both AS and DS can explain in principle the angle profiles observed at low temperatures. However as pointed out in reference [4], neither AS nor DS alone can explain the magnetic field dependence of the oscillation amplitude in the whole field range 0 T $\leq B \leq$ 9 T. Therefore, a more realistic picture of the thermal transport should take both into account. As argued in reference [27], this scenario produces different regimes influenced by the predominance of either the DS or the AS in the magnetic field dependence. Thus, at constant temperature the strength of the magnetic field becomes the parameter that changes the regime. At low magnetic fields the DS dominates and the AS dominates at high fields [27,4]. In both cases, an increase of the oscillation amplitudes with increasing magnetic field strength is predicted. In Figure 3 the oscillation amplitudes of the

thermal conductivity at 3 T and 8 T for different temperatures in the twinned crystal are shown.

As the temperature increases the fourfold oscillation is no longer observable, see Figures 3 and 4. This fact can be understood if one takes into account the thermal activation of the quasiparticles at different orientations from those of the nodes of the order parameter. In other words, if we suppose that the same processes that govern the thermal transport at low temperatures (AS and DS) are responsible for the high temperature behavior as well, we have to conclude that an increasing number of carriers appears in the direction of the heat current as the temperature is raised. As we shall see below from the numerical results using the AS model, this is, in fact, what takes place as the temperature is increased. However, although the observed angle profiles can be well described by the numerical analysis, the amplitude of the oscillations are smaller than the simulation results at $T > 30$ K. As argued for the peak of the curves in Figure 2 and shown in the following section, this discrepancy can be solved by the inclusion of an inelastic scattering into the calculations [13,17].

In Figure 4 we show the angle dependence of the untwinned crystal at 8 T. Similar angle profiles as for the twinned sample have been found, but the amplitude of the oscillation is considerably smaller. This can be explained in terms of a larger concentration of impurity scatterers in the untwinned sample, as discussed above and in reference [11]. In fact, if the impurity scattering rate is sufficiently large, the relative weight of the directionality of the AS and DS mechanisms to $\kappa_{xx}(\theta)$ weakens. The influence of the impurity scattering has been considered in the original models by inclusion of an impurity rate [23,24,14,5].

We note also that the symmetry of the $\kappa_{xx}(\theta)-$curves differs slightly for the twinned and untwinned samples at the same absolute or reduced temperature. The effect of impurity scatterers can be accounted for by an impurity dependent gap parameter as done in reference [23]. In general, however, it can be viewed as an effect related to the ratio of the modulus of the gap and the density of states of the quasiparticles at a temperature T and momentum $\mathbf{p}$. Therefore, since our twinned sample has a larger critical temperature T_c than our untwinned sample, the oxygen deficiency in the latter could be also responsible for a reduced density of states, and therefore, for a different angle patterns respect to the sample with a higher T_c.

Figure 5 shows the complete angle patterns measured in the twinned crystal at 8 T. At $T > 78$ K no clear change in the thermal conductivity when the field is rotated parallel to the CuO_2 planes is observed. This can be explained by taking into account the temperature dependence of the gap, which vanishes at T_c, and the relative increase of the inelastic scattering rate.

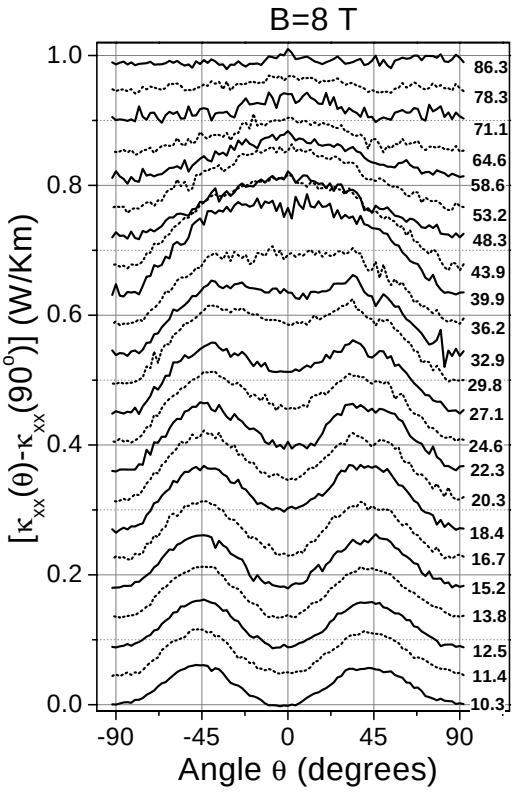

Fig. 5. Angle dependence patterns of the longitudinal thermal conductivity at different temperatures and at 8 T for the twinned sample. The value of the thermal conductivity at $\theta = 90^\circ$ was subtracted to facilitate the comparison with theory. An offset has been added to every curve in order to distinguish the change in the symmetry as the temperature increases.

4 Comparison with the two-dimensional thermal transport theory

To compare the experimental results with theory we take recently published results of the longitudinal and transverse thermal conductivity [4] into account that indicate that at high fields ($B > 2$ T), applied parallel to the planes, the main scattering mechanism for the quasiparticles appears to be the Andreev reflection by vortex supercurrents [25]. Therefore, we use the formulation proposed by Yu *et al.* [5] using a two dimensional model of the BRT expression for the thermal conductivity [8], which has been useful in the interpretation and discussion of previous results [2,11,4]. Under this model the longitudinal thermal conductivity can be written as

$$\kappa_{xx}^{el} = \frac{1}{2\pi^2 c k_B T^2 \hbar^2} \int_{p_F}^{\infty} \mathrm{d}^2 p \frac{v_{gx} v_{gx} E_{\mathbf{p}}^2}{\Gamma(\mathbf{B},\mathbf{p},T)} \mathrm{sech}^2\left(\frac{E_{\mathbf{p}}}{2k_B T}\right), \quad (1)$$

where v_{gx} is the the x-axis component of the group velocity, and $E_{\mathbf{p}}$ is the quasiparticle energy. For this

energy we use a free quasiparticle model $E_{\mathbf{p}}^2 = (\mathbf{p}^2/2m_{\rm eff} - \mu)^2 + \Delta^2(\mathbf{p},T)$ where $m_{\rm eff}$ is the effective mass of the quasiparticle. $\Gamma(\mathbf{B},\mathbf{p},T)$ may be taken as a relaxation rate given by the sum of the following scattering mechanisms acting in series: scattering of QP by impurities $\Gamma_{\rm imp}(\mathbf{p})$, by phonons $\Gamma_{\rm ph}(\mathbf{p},T)$ [18,19,28], by quasiparticles $\Gamma_{\rm qp}(\mathbf{B},\mathbf{p},T)$ [13,29] and AS by vortex supercurrents $\Gamma_v(\mathbf{B},\mathbf{p},T)$ [5]. The expression for this scattering rate according to the model for the AS, proposed by Yu *et al.* [5], is given by

$$\Gamma_v(\mathbf{B},\mathbf{p},T) = \Gamma_v^0 \exp\left\{\frac{-m^2 a_v^2 \left[E_p - |\Delta(\mathbf{p},T)|\right]^2}{p_F^2\hbar^2 \ln(a_v/\xi_0)\sin^2\psi(\mathbf{p})}\right\}, \quad (2)$$

where a_v is the intervortex spacing given in this model by

$$a_v^2 = \frac{p_F^2\hbar^2}{\pi\Delta_0^2\gamma m_e^2}\frac{B_{c2}^{ab}}{B}. \quad (3)$$

We use the BCS-like parameterization for the temperature dependence of the gap amplitude

$$\Delta(T) = \Delta_0 \tanh\left(2.2\sqrt{\frac{T_c}{T}-1}\right), \quad (4)$$

and the $d_{x^2-y^2}$-pairing symmetry in the resulting gap $\Delta(\mathbf{p},T)$ enters as follows

$$\Delta(\mathbf{p},T) = \Delta(T)\left[\frac{\cos(p_x a/\hbar) - \cos(p_y a/\hbar)}{1-\cos(p_F a/\hbar)}\right]. \quad (5)$$

We showed recently [4] that at low temperatures and high fields, a quantitative agreement between this model and the oscillation amplitudes of the thermal conductivity tensor is achieved only if the intervortex spacing is increased by about five times the value defined in equation (3) if we use the parameters from reference [5] ($\Delta_0 = 20$ meV, Ginzburg-Landau parameter $\kappa = 100$, anisotropy $\gamma = 4$, $B_{c2}^{ab} = 650$ T). Furthermore, from those fits [4] for the twinned crystal we obtained a momentum independent impurity scattering $\Gamma_{\rm imp}^{-1} \simeq 0.12$ ps and $(\Gamma_v^0)^{-1}(B = B_{c2}) \simeq (3/2)\Gamma_{\rm imp}^{-1}$. Assuming a total scattering rate given by the sum of the AS and impurity rates, *i.e.* $\Gamma(\mathbf{B},\mathbf{p},T) = \Gamma_v(\mathbf{B},\mathbf{p},T) + \Gamma_{\rm imp}$, the model given by equations (1) to (5) reproduces remarkably well the symmetry of the curves in Figure 5 in the whole measured temperature range. Because in this calculation we do not take explicitly into account the inelastic scattering rate $\Gamma_{\rm in}$ given by phonons $\Gamma_{\rm ph}$ and by quasiparticles $\Gamma_{\rm qp}$, the calculated oscillation amplitude above 20 K increases up to ~ 10 times that observed in the experiment.

In Figure 6 we show the results of the numerical simulation. Each of the curves in this figure has been multiplied by a factor $f(T)$ in order to fit the experimental oscillation amplitude (Fig. 5). We note that the symmetry of the results can be explained quite satisfactorily by this

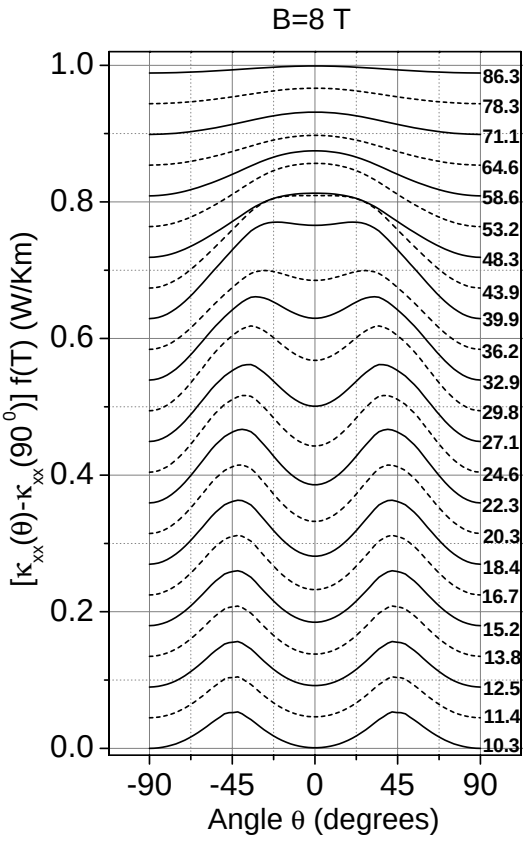

Fig. 6. Angle dependence patterns of the longitudinal thermal conductivity at different temperatures and 8 T calculated using equations (1) to (5) and with parameters given in the text. Each of the curves at a given temperature has been multiplied by a free parameter $f(T)$ in order to fit the experimental oscillation amplitude of the twinned sample. An offset has been added to every curve in order to distinguish the change developed in the symmetry as the temperature increases.

model. This result, on one hand, supports the predominance of $d_{x^2-y^2}$-pairing symmetry of the order parameter up to temperatures close to T_c and, on the other hand, confirms the idea of a competition between the thermal activation of quasiparticles in the direction of the thermal current and the gap structure. We note that the $d_{x^2-y^2}$-gap symmetry is the only gap function that can explain the whole angular patterns up to T_c. Of course, a s-gap also gives a onefold oscillation similar to the experiments above ~ 50 K, but it does produce neither the fourfold oscillation below ~ 15 K nor the curves between 15 K and 50 K. Thus, the set of curves in Figure 5 can be only explained if one uses a main $d_{x^2-y^2}$-gap into the calculations. Furthermore , the anisotropy of d-wave gap proposed for BSCCO [30], does not seem to occur in YBCO since in the latter the nodes are observed at both field orientations $\theta = 45°$ and $\theta = -45°$ (see also references [2,5,4]).

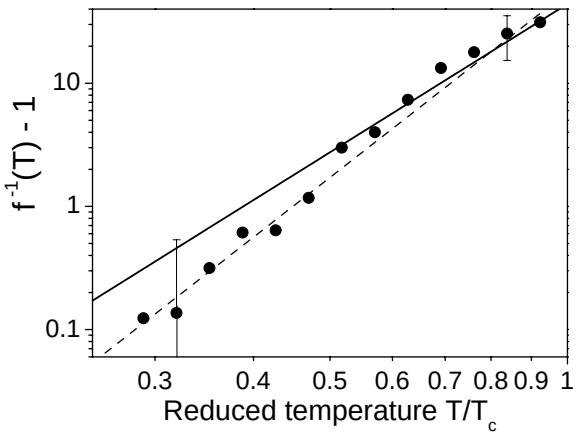

Fig. 7. Temperature dependence of the factor $f^{-1}(T) - 1$ as a function of reduced temperature in a logarithmic scale. The dashed line is a fit of the data to a T^5 dependence and the solid line follows a T^4 dependence.

The factor $f(T)$ is related to the inelastic scattering rate $\Gamma_{\rm in}$, which was not taken explicitly into account in the previous calculations. However, an approximation can be carried out to get roughly the temperature dependence of the total scattering rate, which could be in part associated to the temperature dependence of $\Gamma_{\rm in}$. Since the AS mechanism is weakly temperature dependent below $T/T_c < 0.8$, we may approximate the total scattering rate as

$$\Gamma_{\rm imp} + \Gamma_v + \Gamma_{\rm in} \sim (\Gamma_{\rm imp} + \Gamma_v) f^{-1}(T)\,. \qquad (6)$$

The temperature dependence of the inelastic scattering rate is given then by the factor $f(T)$ in this approximation as

$$\Gamma_{\rm in} \propto f^{-1}(T) - 1\,. \qquad (7)$$

In Figure 7 we plot $f^{-1}(T)-1$. As expected, we recover the overall behavior of the inelastic scattering rate already described by many authors [13,29,18,19,28]. Below T_c it decreases rapidly and becomes negligible in comparison with the impurity and AS scattering rates below ~ 25 K. Although the approximation given by (6) is too rough to obtain the true temperature dependence of the inelastic scattering rate, it is instructive to compare the obtained power dependence with results from literature. Thermal Hall angle measurements performed in the same YBCO twinned crystal show that $\cot(\theta_H) = m_H/\tau_H \propto T^4$ down to ~ 20 K (m_H is the effective mass and τ_H is the Hall scattering time of the quasiparticles responsible for the Hall signal) [10]. The power law dependence obtained for $\tau_H^{-1} \propto T^4$ is similar to that obtained for the longitudinal scattering rate assuming a $d-$wave pairing [20]. Since quasiparticle-quasiparticle scattering mechanism should be the dominant temperature dependent inelastic scattering below T_c, we expect a rate proportional to the density of quasiparticles. Interestingly, within the simple two-fluid model we expect a density of quasiparticles proportional to $(T/T_c)^4$. On the other hand, a T^3 dependence is expected within the spin-fluctuation scattering picture [29].

5 Summary

In summary, we have measured the longitudinal thermal conductivity κ_{xx} in two single crystals of YBCO in the presence of a planar magnetic field which was rotated parallel to the CuO_2 planes, from $T \sim 10$ K up to a few Kelvins below T_c. Fourfold oscillations were recorded below ~ 20 K. Above this temperature the angle dependence of the longitudinal thermal conductivity changes; from the minimum at $\theta = 0°$ (field parallel to the heat current) a maximum develops at high T. The observed behavior in the whole temperature range can be very well reproduced by a model involving Andreev scattering of quasiparticles by vortices and the two-dimensional BRT expression for the thermal conductivity assuming a $d-$wave pairing. The overall results agree with the $d_{x^2-y^2}$-pairing symmetry of the order parameter. This agreement suggests that the mechanisms that influence the behavior of the quasiparticles below T_c and above ~ 10 K are well described by the Fermi liquid theory at nearly optimal doping. The small differences found in the angle patters between the twinned and untwinned samples can be explained in terms of the different impurity concentration as well as oxygen deficiency and are accounted for by the phenomenology exposed in this work.

This work was supported by the DFG under Grant DFG ES 86/4-3.

References

1. C. Tsuei, J. Kirtley, Rev. Mod. Phys. **72**, 969 (2000)
2. H. Aubin, K. Behnia, M. Ribault, R. Gagnon, L. Taillefer, Phys. Rev. Lett. **78**, 2624 (1997)
3. M. Salamon, F. Yu, V.N. Kopylov, J. Superconductivity **8**, 449 (1995)
4. R. Ocaña, P. Esquinazi, Phys. Rev. B **66**, 064525 (2002)
5. F. Yu, M.B. Salamon, A.J. Leggett, W.C. Lee, D.M. Ginsberg, Phys. Rev. Lett. **74**, 5136 (1995)
6. R.A. Klemm, A.M. Goldman, A. Bhattacharya, J. Buan, N.E. Israeloff, C.C. Huang, O.T. Valls, J.Z. Liu, R.N. Shelton, U. Welp, Phys. Rev. Lett. **77**, 3058 (1996)
7. F. Yu, M.B. Salamon, A.J. Leggett, W.C. Lee, D.M. Ginsberg, Phys. Rev. Lett. **77**, 3059 (1996)
8. J. Bardeen, G. Rickayzen, L. Tewordt, Phys. Rev. **15**, 982 (1959)

9. A. Taldenkov, P. Esquinazi, K. Leicht, J. Low Temp. Phys. **115**, 15 (1999)
10. R. Ocaña, A. Taldenkov, P. Esquinazi, Y. Kopelevich, J. Low Temp. Phys. **123**, 181 (2001)
11. R. Ocaña, P. Esquinazi, Phys. Rev. Lett. **87**, 167006 (2001)
12. A. Inyuskin, K. Leicht, P. Esquinazi, Cryogenics **38**, 299 (1998)
13. P. Hirschfeld, W. Putikka, Phys. Rev. Lett. **77**, 3909 (1996)
14. P.J. Hirschfeld, `cond-mat/9809092` (unpublished)
15. C. Kübert, P. Hirschfeld, Phys. Rev. Lett. **80**, 4963 (1998)
16. B. Zeini *et al.*, Eur. Phys. J. B **20**, 189 (2001)
17. D. Bonn *et al.*, Phys. Rev. B **47**, 11314 (1993)
18. M. Houssa, M. Ausloss, Phys. Rev. B **51**, 9372 (1995)
19. M. Houssa, M. Ausloss, Physica C **257**, 321 (1996)
20. R.C. Yu, M.B. Salamon, J.P. Lu, W.C. Lee, Phys. Rev. Lett. **69**, 1431 (1992)
21. B. Zeini, A. Freimuth, B. Büchner, R. Gross, A.P. Kampf, M. Kläser, G. Müller-Vogt, Phys. Rev. Lett. **82**, 2175 (1999)
22. K. Krishana, N.P. Ong, Y. Zhang, Z.A. Xu, R. Gagnon, L. Taillefer, Phys. Rev. Lett. **82**, 5108 (1999)
23. H. Won, K. Maki, `cond-mat/0004105`
24. H. Won, K. Maki, Current Appl. Phys. **1**, 291 (2001)
25. A. Andreev, Sov. Phys. JETP **19**, 1228 (1964)
26. A. Matulis, F.M. Peeters, P. Vasilopoulos, Phys. Rev. Lett. **72**, 1518 (1994)
27. I. Vekhter, A. Houghton, Phys. Rev. Lett. **83**, 4626 (1999)
28. M. Houssa, M. Ausloss, Europhys. Lett. **33**, 695 (1996)
29. S. Quinlan, D. Scalapino, N. Bulut, Phys. Rev. B **49**, 1470 (1994)
30. Y. Ando, J. Takeya, Y. Abe, X. Sun, A. Lavrov, Phys. Rev. Lett. **88**, 147004 (2002)